Metal-Oxide Films Hot Paper

International Edition: DOI: 10.1002/anie.201601647
German Edition: DOI: 10.1002/ange.201601647

Tuning the Reactivity of Ultrathin Oxides: NO Adsorption on Monolayer FeO(111)

Lindsay R. Merte, Christopher J. Heard, Feng Zhang, Juhee Choi, Mikhail Shipilin, Johan Gustafson, Jason F. Weaver, Henrik Grönbeck, and Edvin Lundgren*

Abstract: *Ultrathin metal oxides exhibit unique chemical properties and show promise for applications in heterogeneous catalysis. Monolayer FeO films supported on metal surfaces show large differences in reactivity depending on the metal substrate, potentially enabling tuning of the catalytic properties of these materials. Nitric oxide (NO) adsorption is facile on silver-supported FeO, whereas a similar film grown on platinum is inert to NO under similar conditions. Ab initio calculations link this substrate-dependent behavior to steric hindrance caused by substrate-induced rumpling of the FeO surface, which is stronger for the platinum-supported film. Calculations show that the size of the activation barrier to adsorption caused by the rumpling is dictated by the strength of the metal–oxide interaction, offering a straightforward method for tailoring the adsorption properties of ultrathin films.*

For many years, FeO(111) monolayers grown on platinum surfaces[1,2] were viewed as chemically inert. A number of studies showed weak or negligible adsorption of various molecules, which was attributed to the fact that the polar, oxygen-terminated films do not expose iron ions.[3–6] However, recent work has shown that the FeO films can exhibit catalytic activity for CO oxidation, either because of the presence of exposed iron ions at the edges of films[7] or, at sufficiently high pressures, to thermally activated outward flipping of iron ions.[8–10] Investigations of various supported metal catalysts have shown that similar ultrathin oxide layers form on the metal particles under certain conditions because of so-called strong metal–support interactions (SMSI).[11–13] Although these oxide layers often suppress the catalytic activity of the metal,[14] the novel adsorption properties of the ultrathin oxides themselves allow new possibilities for the development of chemically active materials.[15] To exploit these opportunities, a detailed understanding of the factors that determine the properties of these films is required.

[*] Dr. L. R. Merte, M. Shipilin, Dr. J. Gustafson, Prof. E. Lundgren
Division of Synchrotron Radiation Research
Lund University, 22100 Lund (Sweden)
E-mail: lindsay.merte@sljus.lu.se
Dr. C. J. Heard, Prof. H. Grönbeck
Department of Physics and Competence Centre for Catalysis,
Chalmers University of Technology
41296 Göteborg (Sweden)
Dr. F. Zhang, Dr. J. Choi, Prof. J. F. Weaver
Department of Chemical Engineering
University of Florida, Gainesville, FL 32611 (USA)
Supporting information and the ORCID identification number(s) for the author(s) of this article can be found under http://dx.doi.org/10.1002/anie.201601647.

Although growth of FeO(111) monolayers on metal surfaces other than platinum has been reported,[16–19] these studies have been largely limited to structural characterization and redox properties, and little information about the effect of the substrate on adsorption properties is available. However, there is evidence from published studies that the substrate can influence these properties. For example, the 2.5 nm moiré superstructure of FeO/Pt(111) exhibits inhomogeneous adsorption affinity, and functions as a nanotemplate because of variation in the interface structure within the moiré unit cell.[9,20–23]

A metal substrate can directly influence adsorption on monolayer FeO films by electron exchange, governed by the metal work function and film polarization.[20,24–26] Extensive studies of adsorption on thin films of various oxides have shown that electronic interactions may have drastic effects on the chemical properties of films.[27–31] We carried out the present study to shed light on these effects, using NO as a probe molecule for reactive metal centers,[32] and comparing silver and platinum as support metals. In fact, we observed drastic differences in reactivity between the two substrates; whereas FeO/Pt(111) shows negligible NO uptake at 100 K,[33] NO adsorbs strongly on FeO/Ag(100) under similar conditions, forming a dense monolayer structure that is stable close to room temperature. DFT calculations show that the adsorbed states of NO on the two metal supports are nearly identical. The large difference in reactivity is not directly related to the difference in work functions of the supports, but rather is of kinetic origin. The stronger adhesion of the FeO film to the platinum surface pulls iron ions toward the surface and creates a large barrier to adsorption as a result of steric blocking by the oxygen anions.

A scanning tunneling microscope (STM) image of the FeO(111) film on Ag(100), grown by reactive deposition of iron in a background of O_2, is shown in Figure 1 a.[34] The film exhibits a quasi-hexagonal structure with a moiré modulation arising from coincidence with the substrate. The low energy electron diffraction (LEED) pattern acquired for this film (Figure 1 b) shows reflexes corresponding to the approximate $p(2\times11)$ coincidence structure.

Refinement of the structure was carried out using DFT+U calculations. Models of the optimized structure (Figure 1 c) show the quasi-hexagonal atomic arrangement as well as the polar stacking of the iron and oxygen layers, hereafter referred to as "rumpling", with iron atoms closest to the surface. The average rumpling, calculated as the difference in mean height of the iron- and oxygen-layers, is 0.26 Å, which is roughly one third of the value found for FeO films (ca. 0.7 Å) grown on Pt(111) and Pt(100)[35–37] and is

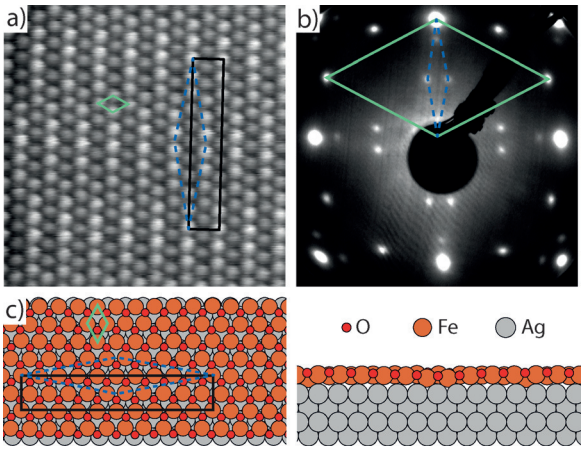

Figure 1. a) STM image (−1 V, 0.2 nA) of monolayer FeO(111) on Ag(100). b) LEED pattern of the FeO film. Beam energy: 60 eV. c) Structural model of the FeO film on Ag(100). Left (top view), right (side view). The basic hexagonal unit cell (green), moiré coincidence cell (dashed blue) and $p(2\times11)$ unit cell used in the computations (black) are indicated, corresponding to the features observed in STM and LEED.

consistent with the expanded in-plane lattice parameter observed for the silver-supported film.[34]

NO adsorption on FeO/Ag(100) was probed experimentally using reflection absorption infrared spectroscopy (RAIRS), temperature-programmed desorption (TPD), and LEED. NO was dosed at 90 K for all measurements. Control experiments on the clean Ag(100) surface under the same conditions showed negligible quantities of NO adsorbing or desorbing, indicating that all NO-related features in the measurements are associated with adsorption onto the iron oxide film.

TPD traces for molecular NO ($m/z = 30$), for a series of increasing NO exposures, show a single dominant feature at 282–295 K that shifts to lower temperature with increasing coverage (Figure 2a). The integrated intensity of the peak grows rapidly with exposure and saturates abruptly at about 2.5 L (inset, Figure 2a). A slight tail to higher temperature is observed for the lowest coverages, which is attributed to the presence of defects such as FeO clusters and step edges. No signals corresponding to N_2, NO_2, or N_2O ($m/z = 28$, 46, 44) could be detected, indicating reversible adsorption and desorption of molecular NO. The integrated TPD intensity at saturation corresponds to a coverage of 1.0 ± 0.2 monolayers with respect to Ag(100), calibrated by comparison with NO desorption from Pd(111),[38] indicating essentially complete saturation of the surface.

RAIRS measurements recorded with increasing NO dose are shown in Figure 2b. Detectable components were observed only within the range between about 1845–1795 cm^{-1}, which we assign to the N–O stretching vibration of a terminal iron nitrosyl complex (Fe-N-O). With increasing coverage, the band shifts to higher frequencies, consistent with intermolecular interactions. At saturation, the band peaks sharply (FWHM = 7 cm^{-1}) at 1843 cm^{-1} and exhibits an asymmetric tail on the low-frequency side.

Based on the large coverage-dependent shift in vibrational frequency and narrow peak at saturation, it is

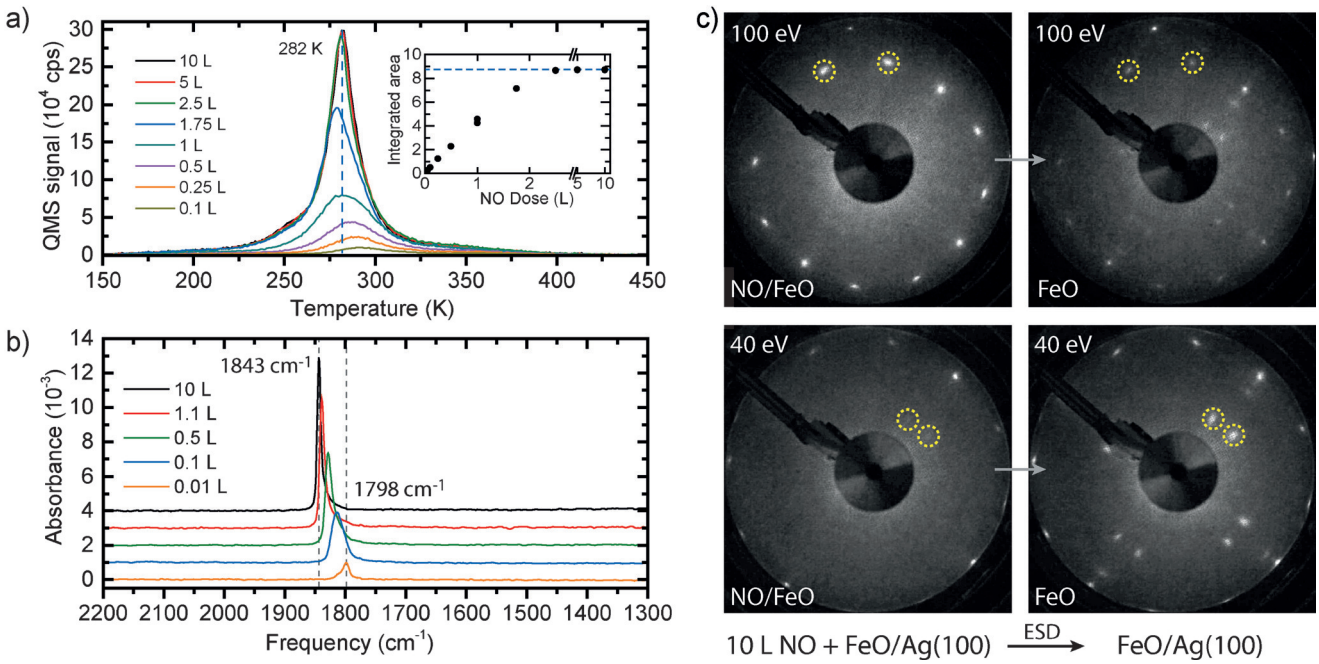

Figure 2. a) Temperature-programmed desorption of NO ($m/z = 30$) from an FeO(111) monolayer on Ag(100) for various NO exposures at 90 K. Inset: a plot of integrated peak areas as a function of exposure. b) Infrared absorption spectra of various coverages of NO on FeO(111)/Ag(100). Peaks are observed in the region corresponding to the N–O stretching mode. c) LEED patterns obtained for the NO-saturated surface (left) at two different beam energies, showing (1×1) symmetry relative to FeO. Exposure to the electron beam led to desorption of NO, with restoration of the pattern of the clean film (right).

concluded that NO forms a dense and uniform monolayer structure. Although the exposures are based on the uncalibrated ion gauge reading, the rate of uptake is consistent in order of magnitude with an initial sticking coefficient of one. LEED patterns of the NO-saturated film at 85 K are shown in Figure 2c. These patterns were acquired at two different beam energies immediately after moving an unexposed part of the sample into the electron beam (left) and after exposure to the electron beam for several seconds (right). At an incident energy of 100 eV, on the NO saturated surface, we observe a (1×1) pattern with respect to FeO(111), with first-order reflexes showing increased intensity compared to the bare film. By comparison, at 40 eV the first-order spots are diminished in intensity and the moiré superstructure reflexes are nearly extinguished. Exposure to the electron beam for about 1 sec restored the LEED pattern of the bare FeO film, indicating that electron-stimulated desorption occurred without significant changes to the structure of the film.

The experimental observations indicate that at 90 K, NO forms a fully saturated (1×1) monolayer, where one NO molecule is adsorbed with an upright geometry on top of each iron ion in the film. The facile adsorption of NO onto the Ag(100) supported FeO film is intriguing, as experiments reported by Lei et al. showed that a similar FeO monolayer grown on Pt(111) is inert to NO adsorption at approximately 100 K.[33] Measurements conducted on FeO/Ag(111) under the same conditions as those described herein showed similar behavior to FeO/Ag(100), indicating that the substrate crystal orientation plays only a minor role (Supporting Information). To clarify the reasons for the contrasting adsorption properties of the silver and platinum supported films, DFT + U calculations were performed for NO adsorption on FeO supported on Pt(111) and Ag(100).

The FeO(111)/Pt(111) system was modeled with a pseudomorphic cell corresponding to the "fcc" domain of the measured $(\sqrt{91}\times\sqrt{91})$R5.2° surface cell,[9] whereas the experimental $p(2\times11)$ cell was considered for FeO(111) supported on Ag(100); see Figure 3a,b. The adhesion energies of the FeO(111) monolayer on the Pt(111) and Ag(100) surfaces were calculated to be 1.36 and 0.46 eV per iron atom.

The significant difference in adhesion energy is reflected in the structural properties of the films. The mean M–Fe interlayer distance is 2.07 Å for FeO(111) supported on Pt(111), whereas it is 2.65 Å for Ag(100). The difference in Fe–M bond strength results in different degrees of rumpling, defined as the average difference in oxygen and iron height above the metal support. As a result of the lattice mismatch, the rumpling varies smoothly over the unit cell for FeO(111) supported on Ag(100) and the average value is calculated to be 0.26 Å. For the pseudomorphic surface cell of FeO/Pt(111), the rumpling is 0.72 Å. Thus, the iron atoms are more exposed to the vacuum when the FeO monolayer is supported on Ag(100), when compared to Pt(111).

NO adsorption was considered on the supported FeO monolayers at coverages of 0.05 and 0.11 for Ag(100) and Pt(111), respectively, in each case corresponding to one NO molecule per supercell. NO adsorbs to iron in a vertical, N-down mode. The NO stretching frequency calculated for

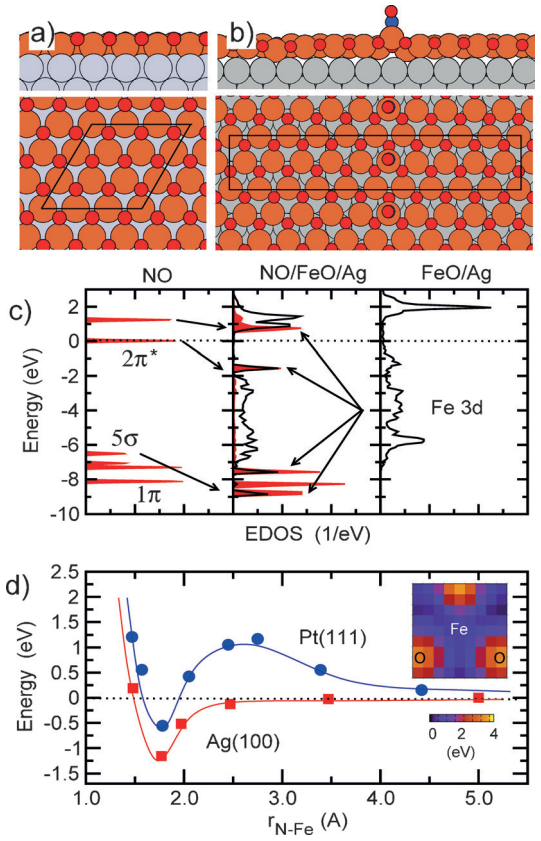

Figure 3. a) Top and side views of FeO(111)/Pt(111). b) Top and side views of FeO(111)/Ag(100) with NO adsorbed at 0.05 coverage. c) Density of states projected onto atomic N, O, and Fe orbitals for (left to right) gas-phase NO, NO/FeO/Ag(100), and FeO/Ag(100). For gas-phase NO, the energy is given with respect to the HOMO level, whereas it is reported with respect to the Fermi energy for the surface systems. d) Potential energy curves for NO adsorption over FeO/Pt(111) and FeO/Ag(100). Inset: a two-dimensional potential energy map of NO adsorption over an FeO/Pt(111) film constrained at the optimized geometry in the absence of NO. The mapping is performed with NO placed 4.07 Å above the topmost platinum layer, which corresponds to the height in the minimum plus 0.2 Å.

adsorption over FeO/Ag(100) is 1800 cm^{-1}, in excellent agreement with the experiments. The adsorption is found to induce a local rumpling inversion in the FeO monolayer, similar to the one reported previously for O_2 adsorption on FeO(111)/Pt(111).[9] The iron atom bound to NO is pulled through the oxygen layer with a vertical displacement of 0.87 Å (Figure 3b). Despite a substantial adsorption energy of 1.16 eV, the N–O bond length is elongated by only 0.01 Å. The local structure of NO adsorbed on FeO/Pt(111) is similar. In this case, the NO-bonded iron atom is also pulled through the film (it is displaced by 1.52 Å) and the N–O bond length is 1.17 Å. However, the adsorption energy is reduced on FeO/Pt(111) to 0.56 eV. The low adsorption energy is primarily due to the loss of the stronger Fe–Pt bonds. Calculations were also performed for the full NO monolayer on FeO/Ag(100) and the local adsorption structure is similar to the low coverage structure (Supporting Information).

NO bonding to the film was analyzed by calculating the projected densities of states (Figure 3c). The projection was

done on atomic nitrogen, oxygen, and iron states for the iron atom bonded to NO. The highest occupied molecular orbital (HOMO) of NO in the gas phase is the $2\pi^*$ state with one electron. The HOMO-1 and HOMO-2 levels are the 5σ and 1π states, respectively. NO adsorption proceeds through hybridization of the π-states with the d_{xz} and d_{yz} orbitals and through the 5σ state with the d_{z^2} orbital. The total occupation of the d_{xz} and d_{yz} orbitals increases from 2.18 to 2.47 electrons upon NO adsorption and the formation of bonding $2\pi^*$-d_{xz} and $1\pi_x$-d_{xz} states. To reduce Pauli repulsion with the 5σ state, there is a simultaneous depletion of charge in the d_{z^2} orbital from 1.65 to 1.21 electrons. Similar types of electronic redistribution occur on the platinum-supported FeO film.

The similarity in the static bonding of NO to FeO(111) supported on silver and platinum suggests that the absence of NO adsorption on FeO/Pt(111) has a kinetic origin. To investigate this possibility, the potential energy curve for NO approaching the FeO(111) surface was evaluated with climbing image nudged elastic band (NEB) calculations. The total energy with respect to the bare films and NO in the gas-phase is shown in Figure 3d. For FeO/Ag(100), the potential energy surface is attractive and has a local minimum at an *N*–Fe distance of 1.78 Å. In contrast, NO encounters a large activation barrier for adsorption on FeO/Pt(111). The barrier is 1.2 eV with a maximum at an *N*–Fe distance of 2.7 Å.

To investigate the origin of the barrier, a two-dimensional potential energy map was calculated for NO adsorption over the FeO/Pt(111) film (inset in Figure 3d). In these calculations, the FeO/Pt(111) system is constrained to the geometry optimized in the absence of adsorbates. Without film relaxation, the potential energy surface is repulsive over the entire cell, and most strongly above the oxygen anions. This confirms the importance of oxygen repulsion in the adsorption process. Therefore, the existence of a substantial barrier for NO adsorption on FeO/Pt(111) can be related to both the larger rumpling, which causes electrostatic repulsion between the NO molecules and the oxygen anions, and the stronger Pt–Fe bond. The iron ion must flip outward before the Fe-NO bond can be formed, requiring breaking of Pt–Fe bonds. In the case of the silver-supported film, the NO molecule may approach the iron ions directly, yielding barrierless adsorption.

In summary, our investigations reveal that the dominant effect determining the reactivity of iron sites in monolayer FeO is the structure of the film, determined by interaction with the underlying substrate. The strong rumpling of the film induced by Pt(111) passivates the oxide through steric hindrance, an effect which is not observed for the more weakly interacting Ag(100) substrate. The presence and size of the activation barrier for adsorption is determined by the strength of the adhesion of the oxide to the metal, offering a straightforward method for controlling the reactivity of FeO. As this substrate-induced rumpling appears to be a general phenomenon for oxide monolayers,[25] we expect these effects to be relevant for a number of catalytically relevant materials.

Acknowledgements

We gratefully acknowledge support of the Röntgen-Ångström cluster "Catalysis on the atomic scale" (Project No. 349-2011-6491) by the Swedish Research Council, as well as the Swedish Foundation for International Cooperation in Research and Higher Education (STINT). The calculations were performed at PDC (Stockholm) and C3SE (Göteborg) thanks to an SNIC grant. J.F.W. gratefully acknowledges financial support provided by the Department of Energy, Office of Basic Energy Sciences, Catalysis Science Division through Grant DE-FG02-03ER15478.

Keywords: heterogeneous catalysis · nitric oxide · oxide films · surface chemistry

How to cite: *Angew. Chem. Int. Ed.* **2016**, *55*, 9267–9271
Angew. Chem. **2016**, *128*, 9413–9417

[1] G. H. Vurens, M. Salmeron, G. A. Somorjai, *Surf. Sci.* **1988**, *201*, 129–144.
[2] H. C. Galloway, J. J. Benitez, M. Salmeron, *Surf. Sci.* **1993**, *298*, 127–133.
[3] Y. Joseph, C. Kuhrs, W. Ranke, M. Ritter, W. Weiss, *Chem. Phys. Lett.* **1999**, *314*, 195–202.
[4] Y. Joseph, M. Wühn, A. Niklewski, W. Ranke, W. Weiss, C. Wöll, R. Schlögl, *Phys. Chem. Chem. Phys.* **2000**, *2*, 5314–5319.
[5] C. Lemire, R. Meyer, V. E. Henrich, S. Shaikhutdinov, H.-J. Freund, *Surf. Sci.* **2004**, *572*, 103–114.
[6] Y. K. Kim, Z. Zhang, G. S. Parkinson, S.-C. Li, B. D. Kay, Z. Dohnalek, *J. Phys. Chem. C* **2009**, *113*, 20020–20028.
[7] Q. Fu, W.-X. Li, Y. Yao, H. Liu, H.-Y. Su, D. Ma, X.-K. Gu, L. Chen, Z. Wang, H. Zhang, B. Wang, X. Bao, *Science* **2010**, *328*, 1141–1144.
[8] Y.-N. Sun, L. Giordano, J. Goniakowski, M. Lewandowski, Z.-H. Qin, C. Noguera, S. Shaikhutdinov, G. Pacchioni, H.-J. Freund, *Angew. Chem. Int. Ed.* **2010**, *49*, 4418–4421; *Angew. Chem.* **2010**, *122*, 4520–4523.
[9] L. Giordano, M. Lewandowski, I. M. N. Groot, Y.-N. Sun, J. Goniakowski, C. Noguera, S. Shaikhutdinov, G. Pacchioni, H.-J. Freund, *J. Phys. Chem. C* **2010**, *114*, 21504–21509.
[10] L. Giordano, G. Pacchioni, C. Noguera, J. Goniakowski, *ChemCatChem* **2014**, *6*, 185–190.
[11] A. K. Datye, D. S. Kalakkad, M. H. Yao, D. J. Smith, *J. Catal.* **1995**, *155*, 148–153.
[12] M. G. Willinger, W. Zhang, O. Bondarchuk, S. Shaikhutdinov, H.-J. Freund, R. Schlögl, *Angew. Chem. Int. Ed.* **2014**, *53*, 5998–6001; *Angew. Chem.* **2014**, *126*, 6108–6112.
[13] T. Lunkenbein, J. Schumann, M. Behrens, R. Schlögl, M. G. Willinger, *Angew. Chem. Int. Ed.* **2015**, *54*, 4544–4548; *Angew. Chem.* **2015**, *127*, 4627–4631.
[14] S. J. Tauster, *Acc. Chem. Res.* **1987**, *20*, 389–394.
[15] H.-J. Freund, G. Pacchioni, *Chem. Soc. Rev.* **2008**, *37*, 2224–2242.
[16] D. Bruns, I. Kiesel, S. Jentsch, S. Lindemann, C. Otte, T. Schemme, T. Kuschel, J. Wollschläger, *J. Phys. Condens. Matter* **2014**, *26*, 315001.
[17] G. Ketteler, W. Ranke, *J. Phys. Chem. B* **2003**, *107*, 4320–4333.
[18] N. A. Khan, C. Matranga, *Surf. Sci.* **2008**, *602*, 932–942.
[19] H. Zeuthen, W. Kudernatsch, G. Peng, L. R. Merte, L. K. Ono, L. Lammich, Y. Bai, L. C. Grabow, M. Mavrikakis, S. Wendt, F. Besenbacher, *J. Phys. Chem. C* **2013**, *117*, 15155–15163.
[20] N. Nilius, E. D. L. Rienks, H. P. Rust, H.-J. Freund, *Phys. Rev. Lett.* **2005**, *95*, 066101.
[21] X. Lin, N. Nilius, *J. Phys. Chem. C* **2008**, *112*, 15325–15328.

[22] L. R. Merte, R. Bechstein, G. Peng, F. Rieboldt, C. A. Farberow, H. Zeuthen, J. Knudsen, E. Lægsgaard, S. Wendt, M. Mavrikakis, F. Besenbacher, *Nat. Commun.* **2014**, *5*, 4193.
[23] L. R. Merte, Y. Bai, H. Zeuthen, G. Peng, L. Lammich, F. Besenbacher, M. Mavrikakis, S. Wendt, *Surf. Sci.* **2016**, DOI: 10.1016/j.susc.2015.12.031.
[24] L. Giordano, G. Pacchioni, J. Goniakowski, N. Nilius, E. D. L. Rienks, H.-J. Freund, *Phys. Rev. Lett.* **2008**, *101*, 026102.
[25] J. Goniakowski, C. Noguera, *Phys. Rev. B* **2009**, *79*, 155433.
[26] J. Goniakowski, C. Noguera, L. Giordano, G. Pacchioni, *Phys. Rev. B* **2009**, *80*, 125403.
[27] G. Pacchioni, H. Freund, *Chem. Rev.* **2013**, *113*, 4035 – 4072.
[28] H. Grönbeck, *J. Phys. Chem. B* **2006**, *110*, 11977 – 11981.
[29] P. Frondelius, A. Hellman, K. Honkala, H. Häkkinen, H. Grönbeck, *Phys. Rev. B* **2008**, *78*, 085426.
[30] G. Barcaro, A. Fortunelli, G. Granozzi, *Phys. Chem. Chem. Phys.* **2008**, *10*, 1876 – 1882.
[31] N. Nilius, M. V. Ganduglia-Pirovano, V. Brázdová, M. Kulawik, J. Sauer, H.-J. Freund, *Phys. Rev. B* **2010**, *81*, 045422.
[32] K. Otto, M. Shelef, *J. Catal.* **1970**, *18*, 184 – 192.
[33] Y. Lei, M. Lewandowski, Y.-N. Sun, Y. Fujimori, Y. Martynova, I. M. N. Groot, R. J. Meyer, L. Giordano, G. Pacchioni, J. Goniakowski, C. Noguera, S. Shaikhutdinov, H.-J. Freund, *ChemCatChem* **2011**, *3*, 671 – 674.
[34] L. R. Merte, M. Shipilin, S. Ataran, S. Blomberg, C. Zhang, A. Mikkelsen, J. Gustafson, E. Lundgren, *J. Phys. Chem. C* **2015**, *119*, 2572 – 2582.
[35] Y. J. Kim, C. Westphal, R. X. Ynzunza, H. C. Galloway, M. Salmeron, M. A. Van Hove, C. S. Fadley, *Phys. Rev. B* **1997**, *55*, R13448 – R13451.
[36] S. Shaikhutdinov, M. Ritter, W. Weiss, *Phys. Rev. B* **2000**, *62*, 7535 – 7541.
[37] L. R. Merte, L. C. Grabow, G. Peng, J. Knudsen, H. Zeuthen, W. Kudernatsch, S. Porsgaard, E. Lægsgaard, M. Mavrikakis, F. Besenbacher, *J. Phys. Chem. C* **2011**, *115*, 2089 – 2099.
[38] P. J. Chen, D. W. Goodman, *Surf. Sci. Lett.* **1993**, *297*, L93 – L99.

Received: February 18, 2016
Revised: April 20, 2016
Published online: June 27, 2016

